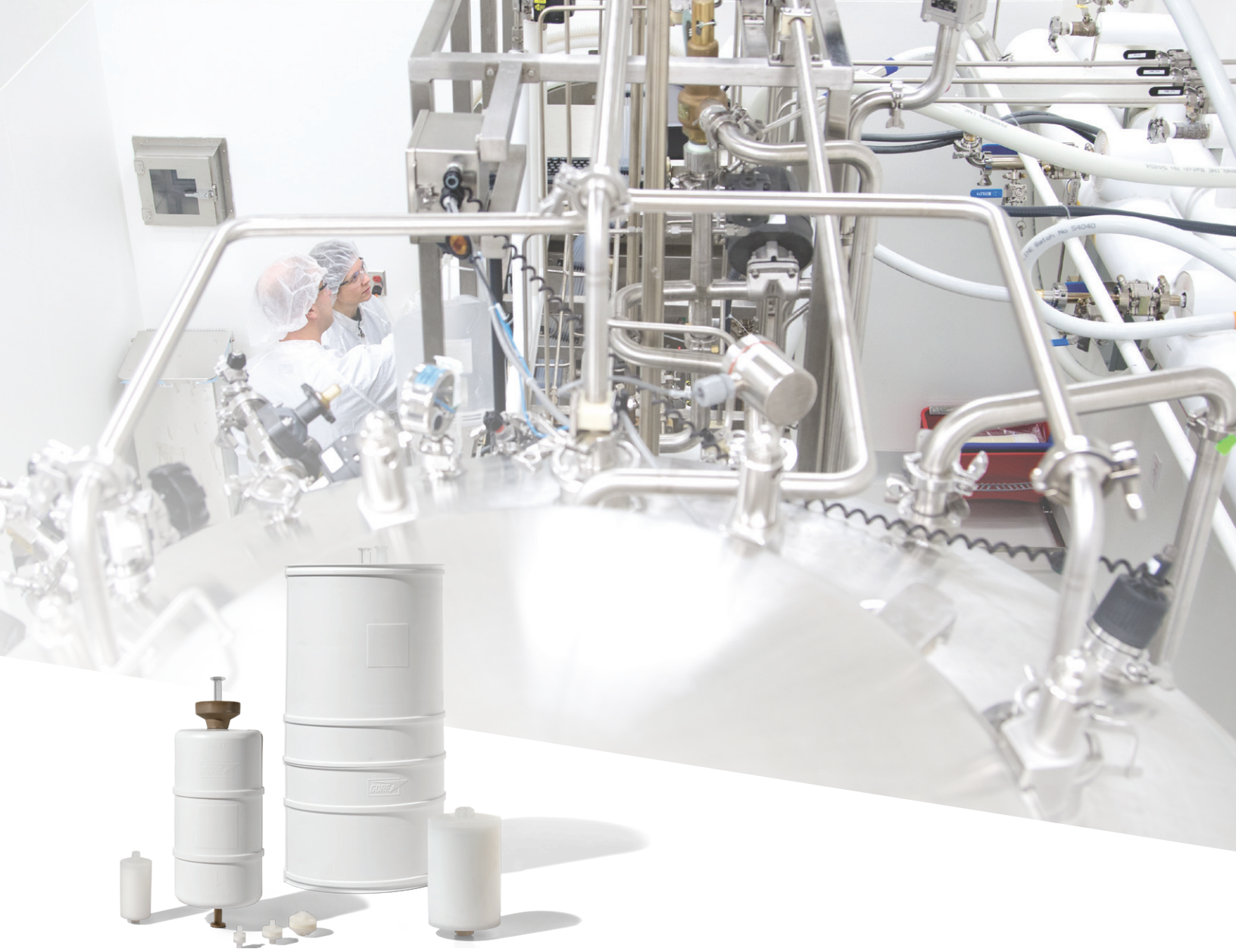

Technical Note

Hydrodynamic Shear and Turbulent Flow Considerations for High Productivity Membrane Affinity Chromatography

AGC Biologics

GORE

Eric Van Voorhees, Hasan Hashemisohi, Ph. D., W.L. Gore and Associates, Inc.
Neha Saxena, Ph.D., Shunsuke Shiina, Ph.D., Rodrigo Gonzalez, Ph. D., AGC Biologics Inc.

Background and Objective

During the manufacturing process, therapeutic antibodies are exposed to a range of hydrodynamic forces and material contact surfaces that can potentially impact protein stability and propensity for aggregation. These forces can vary as fluid flow rates and component design elements scale alongside batch size.

By design, membrane-based affinity chromatography devices enable short residence time, high productivity purification compared to traditional packed-bed affinity resin columns. These attributes can result in comparatively high volumetric flow rates for a given column bed volume and associated flow distribution components. Two intuitive concerns can arise related to the magnitude of forces on proteins and resultant effect on their quality: a) impact of large fluid velocity gradients that impart shear force and b) impact of possible turbulent flow regimes creating additional forces above those caused by the mean flow.

The transition from laminar to turbulent flow is typically quantified by calculating the Reynolds number (Re) from fluid properties, fluid flow rates and design geometry. The laminar/turbulent transition typically occurs above a Re of about 2900. Higher volumetric flow rates in smaller diameter tubing drive higher Re and associated turbulence. However, there is comparatively little emphasis on the effect of turbulent flow on proteins in the research literature. Citing both the size scales of proteins and enzymes relative to the Kolmogorov length scale of turbulence, as well as relatively low kinetic energy of eddies, it has been stated that turbulence is not in and of itself a significant issue regarding proteins.[1] Nonetheless, Re values for flow rates, bed characteristics and design elements typical of membrane chromatography can be quantified and compared to established resin chromatography configurations for reference.

Conversely, a much more studied concern is hydrodynamic shear and its potential impact to the structural destabilization of proteins; specifically, fragmentation, small-scale aggregation (dimers, trimers, etc.) and large-scale aggregation. The impact of shear can be felt across multiple unit operations in bioprocessing (mixing, pumping, filtration, etc.). The shear rate is calculated by the fluid velocity gradient perpendicular to the flow direction while the shear stress is calculated as the product of shear rate and viscosity. Computational Fluid Dynamics (CFD) can be useful in determining shear rates and their distributions in complex systems. For reference, the low end of shear rates in bioprocessing is reported to be on the order of 50 s^{-1} during mixing processes (lasting for minutes to hours) while the high end of shear rates are reported at 10,000-20,000 s^{-1} during filtration and filling operations (lasting for milliseconds to a few seconds).[2] The duration of shear is important in determining any potential impact to protein quality.

Importantly, recent work has established a general consensus that shear alone, in absence of interfaces, is highly unlikely to affect the quality of representative proteins. Experimental studies have shown that globular proteins remain stable even in the presence of shear rates as high as 2×10^5 s^{-1}.[3,4] In fact, theoretical calculations suggest extreme shear rates on the order of 10^7 s^{-1} would be required to unfold proteins.[4] However, the presence of air/water or solid/water interfaces can be a significant factor to the degradation of proteins when in combination with fluid flow.[5-10] Extreme levels of shear can result in cavitation, where air-water interfaces can generate forces sufficient to denature proteins. More likely relevant to chromatography operations are the synergistic effects of solid-liquid interfaces in the presence of hydrodynamic flow, again considering the duration of shear stresses.

Several studies have incorporated the use of parallel plate rheometers with protein solutions to apply controlled shear stress over controlled time intervals in the presence of solid-liquid interfaces. The proteins are subsequently characterized for fragmentation and aggregation. One such study[2] examined shear rates of 20,000 s^{-1} for durations of 300 seconds and 1800 seconds across several monoclonal antibodies (mAbs) and buffer solutions. The levels of this testing were intended to "demonstrate a worst-case, forced-degradation scenario" in context of expected bioprocessing conditions. Subsequent Size Exclusion Chromatography with Multiple Angle Light Scattering (SEC-MALS) and Dynamic Light Scattering (DLS) analysis of the protein solutions after shear exposures suggested

that the "formation of small aggregates is not associated with stresses induced in all conditions." Another study similarly concluded there was no significant increase in soluble intermediate aggregates (dimer, trimer, larger forms) as assessed by SEC.[7] Moreover, there was no evidence that shear resulted in antibody fragmentation.

Conversely, several studies confirm that a population of larger size, subvisible (<2-100 µm) particles can be detected under high shear, long duration conditions in the presence solid-liquid interfaces.[6,7] It is generally hypothesized that the formation of these larger species can be associated with a) protein adsorption to surfaces leading to partial unfolding, desorption and rapid aggregation, b) gradual formation of protein films that can be partially broken and dislodged by the mechanical forces of flow or c) a combination of both.[2] Over longer time periods, these effects can result in measurable loss of monomer concentration.[7]

With the above literature references in mind, the objective of this work was to calculate hydrodynamic shear rate, cumulative shear stress and Reynolds number values that might be expected in high productivity affinity membrane chromatography as a function of size and scale. It was then desired to benchmark these values by performing similar calculations on resin bead columns at representative conditions for comparison. Further, it was desired to experimentally purify a representative clarified CHO cell harvest across several membrane and resin column size scales to compare low order protein aggregation and/or fragmentation profiles. The experiments would also evaluate whether elution yields and/or column fouling would be practically impacted by any large-scale aggregation taking place at solid phase interfaces over repeated cycling.

Experimental

Structure characterization and flow simulation

To calculate flow and shear parameters in the various components of both membrane and resin chromatography systems, structure characterization and Computational Fluid Dynamics (CFD) simulations were performed.

To represent membrane affinity chromatography technology, GORE® Protein Capture Devices with Protein A (GPCD) were evaluated. The membrane structure within these devices was characterized by performing 3-D X-ray Computed Tomography (CT) scans (nano3DX, Rigaku Analytical Devices) at a resolution of 0.325 µm with subsequent segmentation. The segmented images were then reconstructed via image processing (Avizo, Thermo Fisher Scientific Inc.) to create and export 3D models. The fluid domain through porous media was extracted from the 3D structures. A 200 μm^3 sample volume was chosen for the fluid simulations. The flow rate through the membrane was calculated based on a 10 second residence time (SRT) and a nominal bed height of 0.8 cm.

The material modeling software GeoDict (Math2Market GmbH) was used to generate the 3D porous structure model representing the resin bead packed bed. To characterize a representative resin structure, an 85 µm nominal size resin particle was packed randomly to reach a 31% extra particle porosity. A 1 mm^3 sample volume was chosen for the fluid simulations. The flow rate through the resin was calculated based on a 3-minute residence time (MRT) through a 20 cm bed height.

Flow simulations were performed in the commercial CFD solver Simcenter STAR-CCM+ (Siemens Digital Industries Software) to determine the flow field and calculate the shear stresses. The fluid flow solver is based on the finite volume method where the flow domain is divided into smaller volumes (cells), and the governing equations are solved at the centroid of each cell. The fluids were modeled as Newtonian, given that they were aqueous based and of low dissolved solids concentration, so that the shear stress is proportional to the strain rate. A no-slip condition was prescribed on the walls. The flow fluid velocity in the three directions is computed from solving the governing equations.

Reynolds number calculations and numerical methods for shear rate determination

Reynolds numbers (Re) within the chromatographic media bed and fluid distribution components for both membrane devices and packed bed resin columns were calculated from Equation 1:

Equation 1: $Re = \rho VD/\mu$

Where: ρ = fluid density, V = fluid velocity magnitude, D = characteristic diameter, μ = fluid viscosity

Given the use of aqueous based buffer systems, fluid density and viscosity values for water were assumed for all Equation 1 calculations. The average pore diameter for both the membrane and packed resin bed were determined from the structure characterization and subsequently used for the respective characteristic diameters. The CFD simulations were used to determine the respective fluid velocity magnitudes.

Fluid shear rate magnitudes within the chromatographic media bed and fluid flow components were determined from the spatial velocity distributions determined with CFD. Shear stress is then represented by the product of shear rate and dynamic viscosity. Further, streamlined-based integration techniques were used to quantify the *cumulative* shear stress through the bed and components. Specifically, the paths of individual fluid particles were traced along different streamlines and the shear stress was numerically integrated over the appropriate dimensions. This integration process, conducted within the CFD simulation framework, enabled the determination of the cumulative effect of shear stress from the inlet to the outlet.

Protein A membrane chromatography

For the experimental testing of membrane affinity chromatography technology, three membrane bed volume sizes of Gore Protein Capture Devices were evaluated: 3.5 mL, 232 mL and 2 L. The 2 L device was configured by parallel manifolding two 1 L devices. These devices represent bed volumes capable of laboratory evaluation to clinical scale manufacturing. All GPCDs incorporate the same composite ePTFE based membrane that enable high binding capacity at fast flow rates in a pre-packed format.

All device sizes were used to process the same nominal monoclonal antibody (mAb) expressing CHO cell culture harvest clarified using a two-stage cartridge depth filter followed by a 0.2 μm capsule sterile filtration. A 90 L culture harvest batch size was processed in the 232 mL GPCD evaluation while a 500 L culture harvest batch size was processed in the 3.5 mL and 2 L GPCD evaluations.

Table 1 summarizes the nominal harvest cycling protocol used for the three device sizes, with variations footnoted.

Table 1. Nominal harvest cycling protocol for Gore Protein Capture Devices

Step	Fluid	Step Duration (MV)	Residence Time (min)
Equilibration	Tris-HCl buffer	3.00[1]	0.20
Load	Cell culture harvest	80% of $DBC_{10\%}$	0.40
Wash 1	Tris-HCl Buffer	1.43	0.40
Wash 2	Tris-HCl + NaCl buffer	3.00	0.20
Pre-elution wash	Tris-HCl buffer	3.00	0.20
Elution	Sodium Acetate buffer	3.75	0.20[3]
Clean in Place (CIP)	0.1N NaOH	3.00[2]	0.40
Re-Equilibration	Tris-HCl Buffer	3.00	0.20

1. Up to 7 MV for first 5 cycles for 232 mL device
2. 5 MV used for cycles 1-10 for 2 L device
3. 0.33 MRT for first 5 cycles for 232 mL device

The load volume reflected an estimated Dynamic Binding Capacity at 10% Breakthrough ($DBC_{10\%}$) of 25 g/L at 24 seconds residence time (SRT) based on prior, unpublished work with this molecule using a 1 mL Gore membrane device.

The 3.5 mL device was cycled nine times, while the 232 mL and the 2 L devices were both cycled 19 times using appropriately scaled liquid chromatography equipment.

Protein A resin capture reference

To establish benchmark critical quality attribute targets for the Protein A capture step, the same cell culture harvest lot used in the 3.5 mL and 2 L GPCD evaluation was purified using a 5 mL HiTrap MabSelect SuRe™ Protein A resin column (Cytiva). This column was cycled four times using the same buffer scheme and cycling steps that are detailed in Table 1 except that a) all steps were performed at a 3-minute residence time and b) loading DBC was estimated at 30 g/L based on prior, unpublished work with this molecule and resin. Similarly, the same cell culture harvest lot used in the 232 mL GPCD evaluation was purified using a 100 mL MabSelect PrismA™ Protein A resin column (Cytiva), however, this column was only cycled one time.

Analytical

Cell culture harvest mAb concentration was quantified with an Octet RED 96e (FortéBio) using Protein A Dip and Read™ Biosensors. Elution mAb concentrations were measured with a NanoDrop One (Thermo Fisher Scientific, Inc.).

After neutralizing elutions to pH 6-7, product related impurities were quantified using HPLC Size Exclusion Chromatography (SEC) on an Agilent 1100 platform. Products were isocratically separated at a 0.3 ml/min flow rate on a TSKgel® SuperSW mAB HTP column (Tosoh Bioscience) coupled with a Diode Array Detector. Peaks were analyzed to quantify percent of high and low molecular weight species in relation to the target mAb main peak.

Results and Discussion

Reynolds number calculations– chromatographic media bed

Figure 1 illustrates the CFD flow streamlines, color-coded by the fluid velocity, through the resin structure (left, 3-minute residence time) and membrane structure (right, 10-second residence time).

Figure 1. Flow streamlines through resin column (left) and membrane (right), colored by velocity

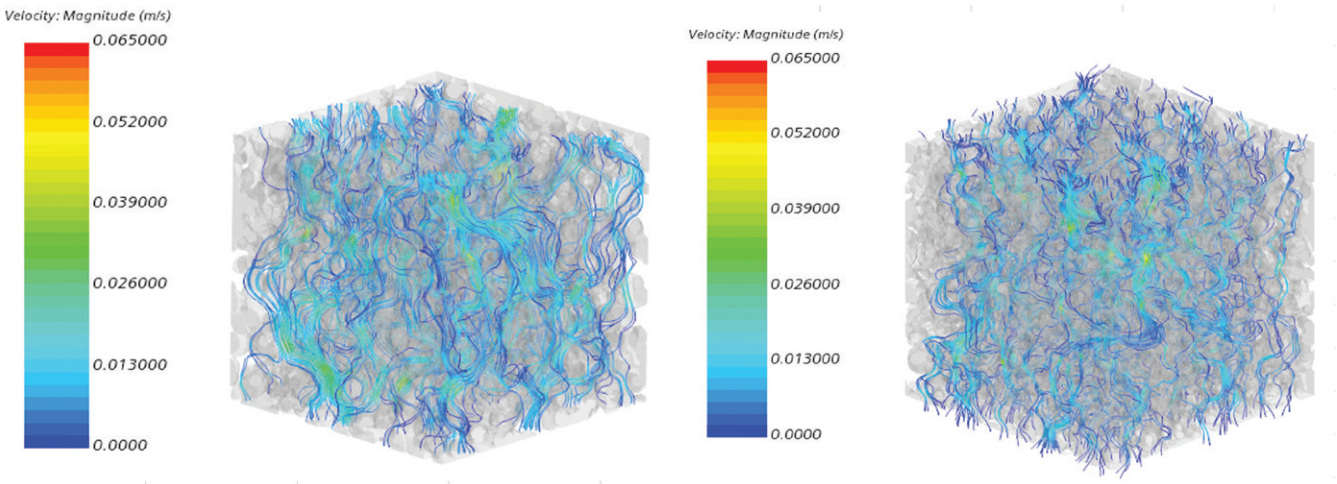

Figure 1 compares the distribution of fluid velocities in the resin and membrane beds. The volumetric average velocity is calculated to be 0.0029 m/s for the resin structure and 0.0017 m/s for the membrane structure, with neither structure exceeding 0.065 m/s. The lower velocities of the membrane structure can be understood in context of significantly shorter bed heights and resultant linear flow rates. When these fluid velocities and characteristic pore dimensions are factored into Equation 1, the Re values of fluid flow at representative flow rates through both membrane and resin structures were less than 1. It can be appreciated that these values are very low and well away from any turbulent flow transition (typically Re 2300–4000). Importantly, these magnitudes are independent of device bed volume for membrane devices.

Reynolds number calculations–inlet and outlet tubing

Table 2 summarizes representative tubing diameters and volumetric flow rates for membrane devices ranging from 3.5 mL to 2 L bed volumes, all from 10 to 30 SRT flow rates. Table 2 also shows tubing and volumetric flow rates for resin columns ranging from 5 mL to 32 L (capable of processing a 2000 L harvest batch) with flow rates ranging from 2 MRT to 4 MRT.

Table 2. Summary of bed volume, tubing ID and volumetric flow rates used in Re calculations

Column type	Bed volume (mL)	Inlet and outlet tubing ID (mm)	Range of volumetric flow rates (mL/min)
Membrane	3.5	1	11-30
	9	1	18-54
	58	3	116-348
	232	6.35	464-1,392
	250	4.78	500-1,500
	1000	9.96	2,000-6,000
	2000	12.7	4,000-12,000
Resin	5	0.5	1.3-2.5
	100	1	25-50
	32,000	19.1	8,000-16,000

Figure 2 graphically summarizes Reynolds Number calculations derived using Equation 1 across a range of representative flow rates (expressed as column residence time) for membrane devices as well as reference resin columns.

Figure 2. Re calculations for flow within tubing as a function of flow rate, with reference to an approximate laminar-to-turbulent flow transition

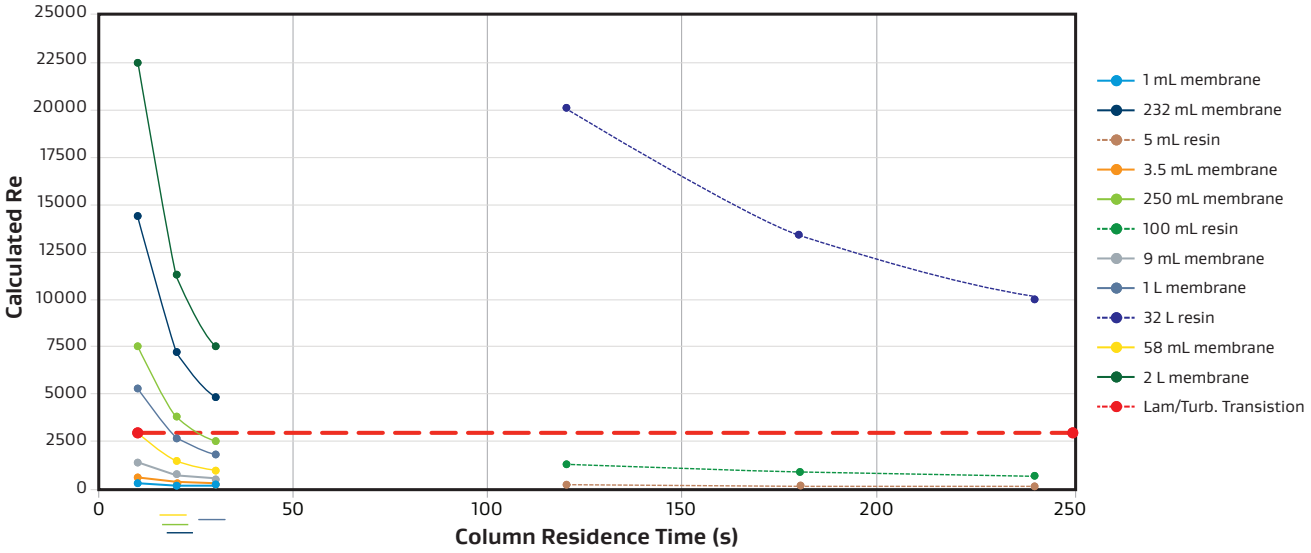

Figure 2 illustrates the relationship between volumetric flow rate on the transition to turbulent flow, highlighting the effect of increasingly larger membrane columns. Note that Re numbers are comparable for both the 2 L membrane column and the 32 L resin column, which are both capable of processing 2000 L bioreactor batch outputs within typical desired time limits.

Shear rate distribution and cumulative shear stress

Figure 3 illustrates model outputs of shear rate calculations in volume elements of the membrane (10 SRT) and resin (3 MRT) porous structures. The histograms beneath each model output summarize the calculated volumetric distribution of the shear rates within the volume element. The results illustrate the volume fraction weighting towards comparatively small shear rates within the chromatographic media bed. Weighted averaging, defined as the sum of the products of volume fraction and shear rate, is a way to reduce the distributions to a single value. For example, the weighted average of the distributions shown in Figure 3 is 937 s^{-1} for the membrane and 291 s^{-1} for the resin bed. These magnitudes of shear rate can be contextualized with the literature values discussed in the Background section[2,3,4].

Figure 3. Shear rate model outputs (top) and calculated volumetric distributions (bottom) are shown for the resin bed (left) and membrane bed (right)

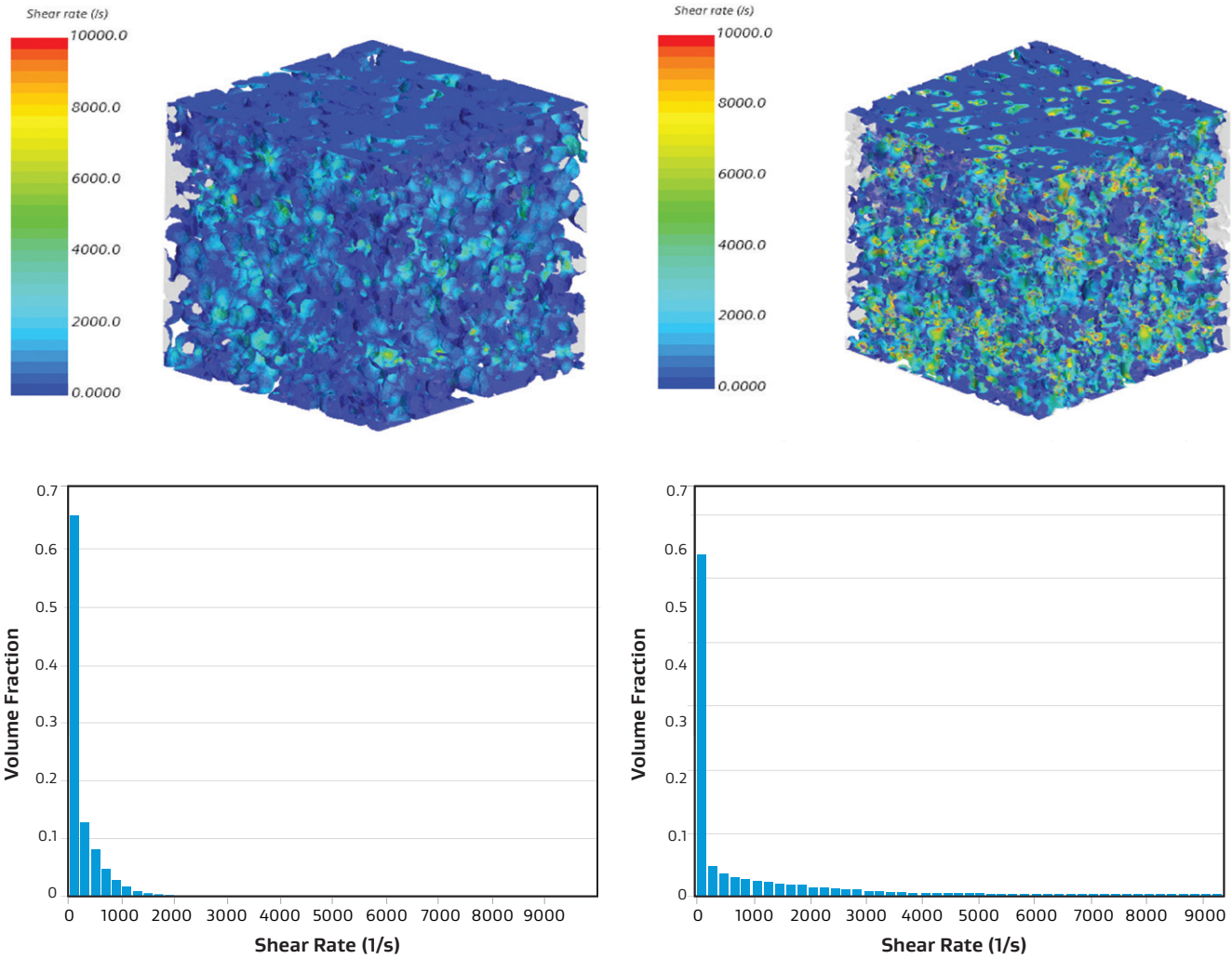

AGC Biologics

GORE

To factor in the duration of the shear, the cumulative shear stress was calculated using the integration method described in the Experimental section. Figure 4 compares histograms of the cumulative shear stress on material passed through the entirety of a resin (3 MRT) and membrane (10 SRT) column, respectively.

Figure 4. Comparison of cumulative shear stress magnitude and distribution of material passed through a resin column (left) and membrane device (right)

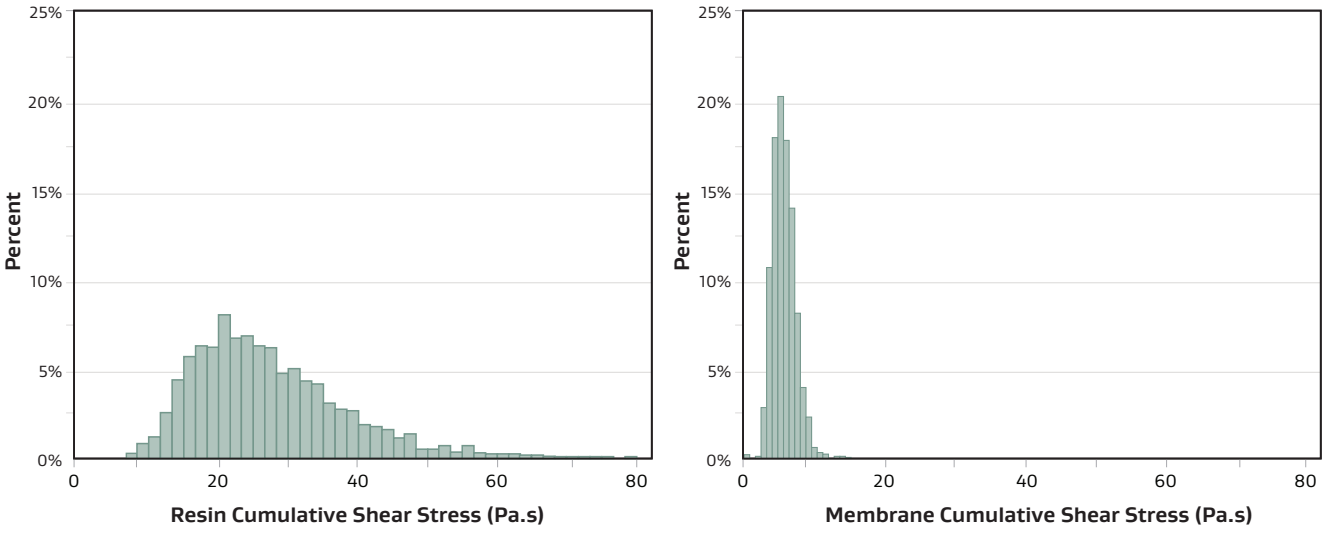

When factoring in the much longer bed length of the resin column, the calculations represented in Figure 4 suggest that despite a higher weighted average shear rate within the membrane bed, there is a lower cumulative shear stress compared to the resin columns.

A similar approach to the above was taken to calculate the shear rate distribution and cumulative shear stress through tubing and fluid distribution elements of different volume devices. By way of example, Figure 5 shows the shear rate model output and volumetric shear rate distribution histogram of the inlet/outlet tubing and flow distributor of a 58 mL membrane device.

Figure 5. Shear rate model output for the tubing and flow distribution elements of a 58 mL membrane device (left) and associated histogram of calculated volumetric shear rate distribution (right)

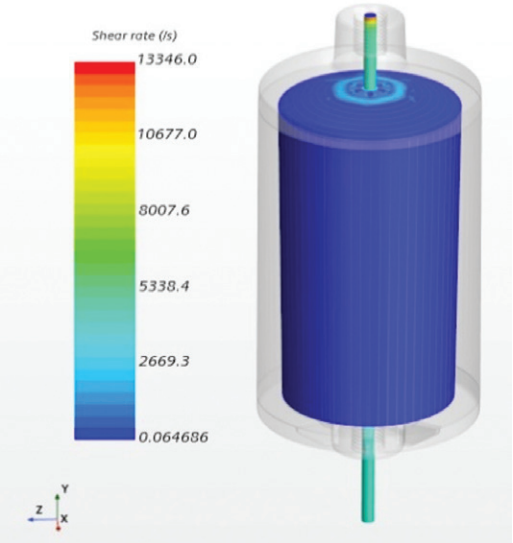

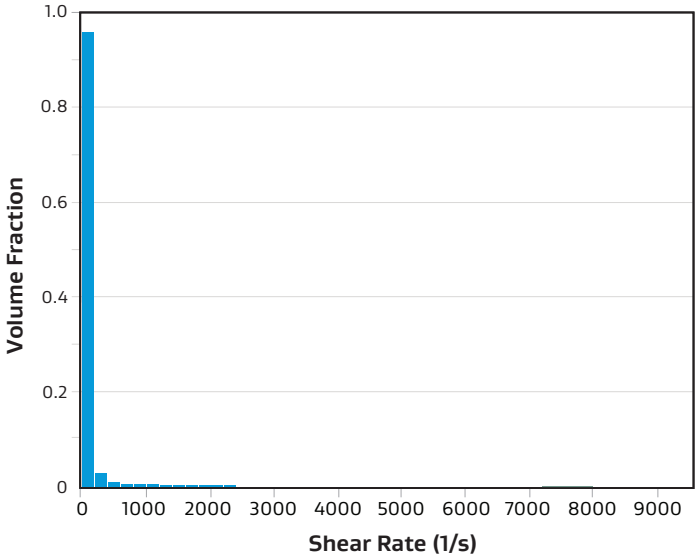

Further, Figure 6 shows a histogram of the calculated cumulative shear stress associated with the tubing and distribution elements of the 58 ml device described in Figure 5.

Figure 6. Cumulative shear stress on the material passed through the tubing and distribution elements of the 58 ml device

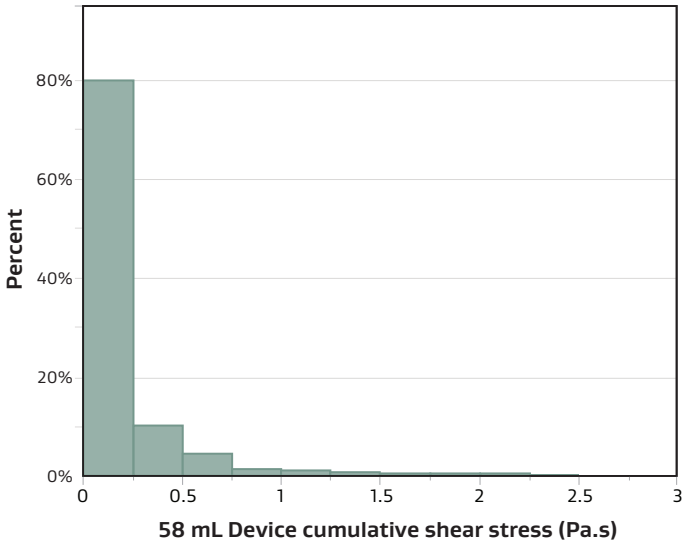

The same approach summarized in Figures 5 and 6 was used across a range of flow elements across a range of membrane device sizes. Table 3 summarizes the average cumulative shear stresses from these calculations. To put perspective to the magnitudes of the flow element shear stresses, Table 3 also shows the average cumulative shear stress values calculated from the membrane and resin chromatographic media beds as detailed in Figure 4.

Table 3. Summary of averaged cumulative shear stress for membrane flow distribution elements across different size scales, including reference averages for both membrane and resin chromatographic media beds

Flow components or bed type modelled	Average cumulative shear stress (Pa.s)
58 ml fluid distributor and tubing	0.29
232 ml fluid distributor, tubing and air trap	0.53
250 ml fluid distributor and tubing	0.39
1 L integrated air trap	1.10
1 L fluid distributor and tubing	0.99
4 L manifold	0.38
Membrane bed	5.68
Resin bed	27.12

The calculations shown in Table 3 illustrate the low cumulative shear stress in typical tubing, air traps and flow distribution elements of membrane chromatography design elements in comparison to those experienced in a resin bed. This can be understood when considering the relatively short residence times of the material inside these elements. Moreover, these magnitudes of cumulative shear stress can be contextualized in the study performed by Bee et. al.[10]

Experimental cycling and impact to protein quality

To experimentally determine the impact of the calculated flow characteristics and shear rate regimes on low order aggregation and/or fragmentation of target proteins, HPLC analysis of the neutralized fractions from cycled membrane devices of various sizes and packed-bed resin columns was performed as described in the Experimental section.

The two graphs in Figure 7 below summarize the percent main peak and percent high molecular weight peak, respectively, from pooled elutions across the three membrane GPCDs. Data from a resin column purifying the same cell culture harvest are shown for reference. Note that low molecular weight peak fractions that are indicative of protein fragmentation were typically < .04% in all cases and are therefore not shown.

Figure 7. Size Exclusion Chromatography results of neutralized elution fractions

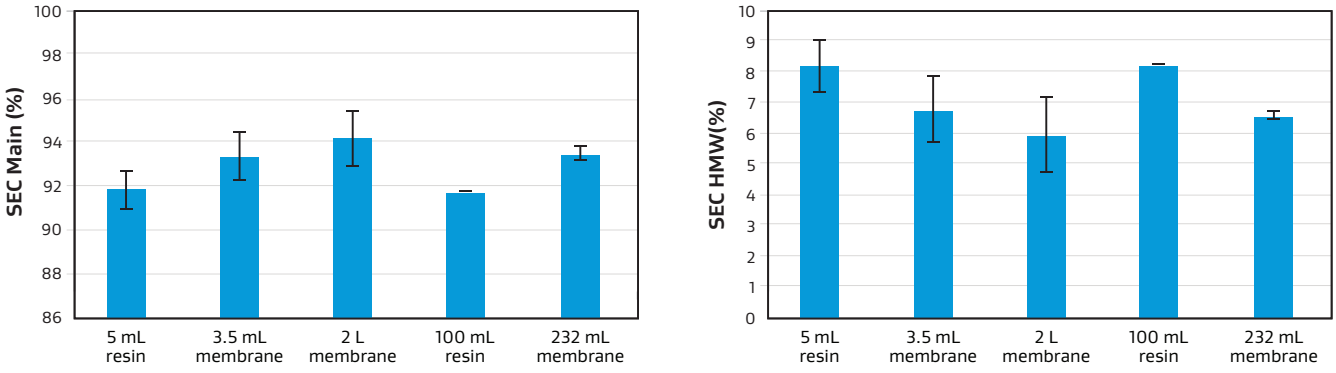

The data in Figure 7 suggest that, on average, the three GPCD sizes showed comparable aggregation profiles spanning the range of shear rates, cumulative shear stress and Re characteristics quantified in the preceding section. Moreover, all three GPCD sizes showed comparable or better profiles vs. the resin column control cycled with a three-minute residence time.

To understand any progressive impact of harvest cycling, the two graphs in Figure 8 below chart the SEC percent main peak and percent high molecular weight peak, respectively, for individual elutions as a function of harvest cycle number.

Figure 8. SEC percent main peak (left) and percent high molecular weight (right) for elutions from individual cycles

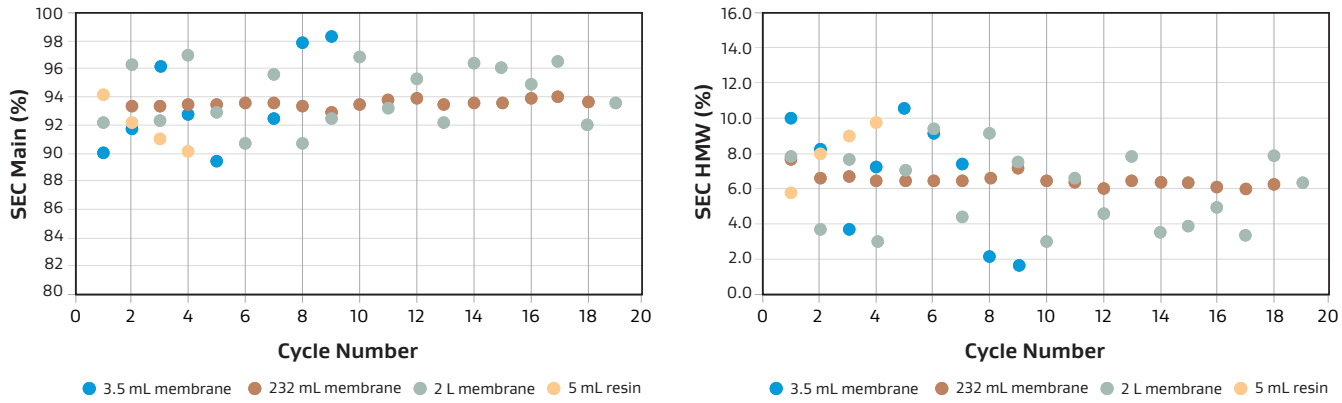

These data suggest that, across all size scales, aggregation profiles show no discernable trending with successive cycles that would be suggestive of progressive protein deposition, denaturing and detaching as small-scale aggregates.

In contrast to the small-scale aggregation quantified by SEC, the possibility of the larger scale protein aggregation and stripping phenomenon described in the Background could conceivably result in either progressive protein yield loss or column pressure rise associated with displaced aggregates occluding the membrane structure.

Figures 9 and 10 chart the measured elution yield and maximum column delta pressure at elution for the 3.5 mL, 232 mL and 2 L membrane devices over their respective cycling.

Figure 9. Elution yield trends for membrane devices as a function of harvest cycling

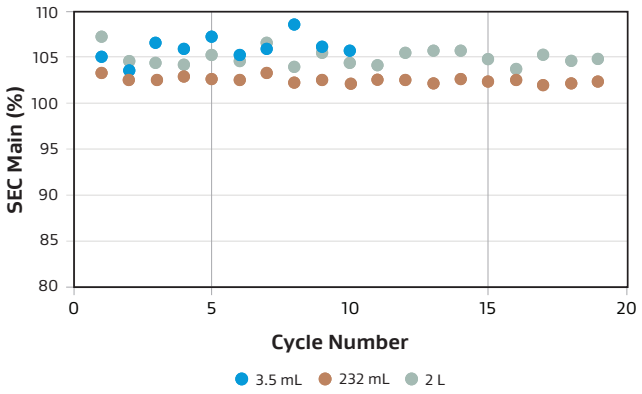

Figure 10. Column delta pressure at elution spike for membrane devices as a function of harvest cycling (all data at 12 SRT flow rate)

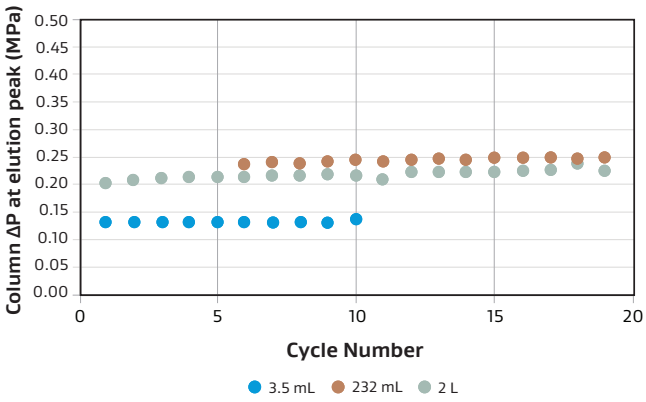

The relatively consistent yield and pressure profiles would not suggest a practically significant loss of target protein or aggregate shedding/column obstruction occurring during harvest cycling. The yield of the resin control was comparable. Calculated yields over 100% are likely a measurement artifact of the two different analytical methods used to determine product concentration in purified eluate vs. clarified harvest fluid.

Conclusions

Structure characterization and computational modeling of fluid flow through a high-productivity affinity membrane bed used in the primary capture of therapeutic proteins suggest extremely low Reynolds numbers that are well away from any turbulent flow regimes. As membrane device sizes increase towards the liter bed volume scale, high volumetric flows in distribution tubing can transition into turbulent flow regimes within the tubing; however, these are of the same order as would be expected in larger benchmark resin columns required to process an equivalent harvest batch size.

The computational modeling approach was further used to calculate shear rate and cumulative shear stress that may be imparted to proteins during both membrane and resin bed affinity chromatography. Although weighted shear rate averages are calculated to be higher within the membrane bed, cumulative shear stress values that factor in column geometry, etc. were found to be lower within the membrane bed vs. a resin bed capable of processing the same volume. Both shear rate and cumulative shear stress values were relatively modest in context of literature research investigating the effects of shear on globular proteins in the presence of interfaces.

Experimental work purifying a representative cell culture harvest across a wide range of membrane column sizes indicated consistent small scale aggregation profiles which were comparable to a resin column control. Moreover, consistent yield and consistent column pressures did not suggest significant large scale aggregation issues related to interfacial shear considerations.

References

1. Thomas, C. R., & Geer, D. (2011). Effects of shear on proteins in solution. Biotechnology Letters, 33(3), 443–456

2. Nanda T., He J., Haas M., Shpungin S., Rusanov I., Sweder R., Brisbane C., and Nesta D., Aggregation from Shear Stress and Surface Interaction: Molecule-Specific or Universal Phenomenon? BioProcess International, 15(4) 2017 30-39

3. Maa, Y.-F., & Hsu, C. C. (1996). Effect of high shear on proteins. Biotechnology and Bioengineering, 51(4), 458–465.

4. Jaspe, J., Hagen, S., Do protein molecules unfold in a simple shear flow? Biophysical Journal, 91 (9), 3415-3424.

5. Grigolato, F., & Arosio, P. (2019). Synergistic effects of flow and interfaces on antibody aggregation. Biotechnology and Bioengineering, 117(2), 417–428.

6. Biddlecombe JG, Smith G, Uddin S, Mulot S, Spencer D, Gee C, Fish BC, Bracewell DG. 2009. Factors influencing antibody stability at solid–liquid interfaces in a high shear environment. Biotechnol Prog 25(5):1499–1507

7. Biddlecombe JG, Craig A., Zhang H., Uddin S., Mulot S., Fish B., Bracewell D., Determining Antibody Stability: Creation of Solid- Liquid Interfacial Effects within a High Shear Environment, Biotechnol. Prog. 23(5) 2007: 1218–1222

8. Perevozchikova, T., Nanda, H., Nesta, D. P., & Roberts, C. J. (2015). Protein adsorption, desorption, and aggregation mediated by solid- liquid interfaces. Journal of Pharmaceutical Sciences, 104(6), 1946–1959

9. Li, J., Krause, M. E., Chen, X., Cheng, Y., Dai, W., Hill, J. J., Huang, M., Jordan, S., LaCasse, D., Narhi, L., Shalaev, E., Shieh, I. C., Thomas, J. C., Tu, R., Zheng, S., & Zhu, L. (2019). Interfacial stress in the development of biologics: fundamental understanding, current practice, and future perspective. The AAPS Journal, 21(3), 44

10. Bee, J. S., Stevenson, J., Mehta, B, Svitel, J., Pollastrinin, J., Platz, R., Freund, E., Carpenter, J. , & Randolph, T. Response of a concentrated monoclonal antibody formation to high shear, Biotechnol Bioeng., 103(5) 2009 936-943.

11. Roffi, K., Li, Li & Pantazis, Jacob, (2021). Adsorbed protein film on pump surfaces leads to particle formation during fill- finish manufacturing, Biotechnol. Bioeng., 118:2947-2957

AGC Biologics

GORE

About AGC Biologics

AGC Biologics is a leading global biopharmaceutical Contract Development and Manufacturing Organization (CDMO) with a strong commitment to delivering the highest standard of service as we work side-by-side with our clients and partners, every step of the way. We provide world-class development and manufacture of mammalian and microbial-based therapeutic proteins, plasmid DNA (pDNA), messenger RNA (mRNA), viral vectors, and genetically engineered cells. Our global network spans the U.S., Europe, and Asia, with cGMP-compliant facilities in Seattle, Washington; Boulder and Longmont, Colorado; Copenhagen, Denmark; Heidelberg, Germany; Milan, Italy; and Chiba, Japan and we currently employ more than 2,500 employees worldwide. Our commitment to continuous innovation fosters the technical creativity to solve our clients' most complex challenges, including specialization in fast-track projects and rare diseases. AGC Biologics is the partner of choice. To learn more, visit agcbio.com.

About Gore

W. L. Gore & Associates is a global materials science company dedicated to transforming industries and improving lives. Since 1958, Gore has solved complex technical challenges in demanding environments — from outer space to the world's highest peaks to the inner workings of the human body. With more than 12,000 associates and a strong, team-oriented culture, Gore generates annual revenues of $4.5 billion. For more information, visit gore.com.

Gore PharmBIO Products

Our technologies, capabilities, and competencies in fluoropolymer science are focused on satisfying the evolving product, regulatory, and quality needs of pharmaceutical and bioprocessing customers, and medical device manufacturers. GORE Protein Capture Devices with Protein A, like all products in the Gore PharmBIO Products portfolio, are tested and manufactured under stringent quality systems. These high-performance products provide creative solutions to our customers' design, manufacturing, and performance-in-use needs.

NOT INTENDED FOR USE in medical device or food contact applications or with radiation sterilization.

All technical information and advice given here is based on our previous experiences and/or test results. We give this information to the best of our knowledge, but assume no legal responsibility. Customers are asked to check the suitability and usability of our products in the specific applications, since the performance of the product can only be judged when all necessary operating data is available. Gore's terms and conditions of sales apply to the purchase and sale of the product.

Americas | W. L. Gore & Associates, Inc.
402 Vieve's Way • Elkton, MD 21921 • USA
Phone: +1 410 506 1715 • Toll-free (US): 1 800 294 4673
Email: pharmbio@wlgore.com

Europe | W. L. Gore & Associates, GmbH
Wernher-von-Braun-Strasse 18 • 85640 Putzbrunn, Germany
Phone: +49 89 4612 3456 • Toll free: 0 800 4612 3456
Email: pharmbio_eu@wlgore.com

gore.com/pharmbio

PB13305-RI-TEC-US-APR24